

Bi-functional air electrode developed from dual-MOFs strategy for high-performance zinc-air batteries

Yasir Arafat ^a, Muhammad Rizwan Azhar ^b, Yijun Zhong ^a, Xiaomin Xu ^a, Moses O Tadé ^a and Zongping Shao ^{*a}

a. WA School of Mines: Minerals, Energy and Chemical Engineering (WASM-MECE), Curtin University, Perth, WA 6102, Australia.

b. School of Engineering, Edith Cowan University, 270 Joondalup Drive, Joondalup, WA 6027, Australia.

*Corresponding author

Supplementary information

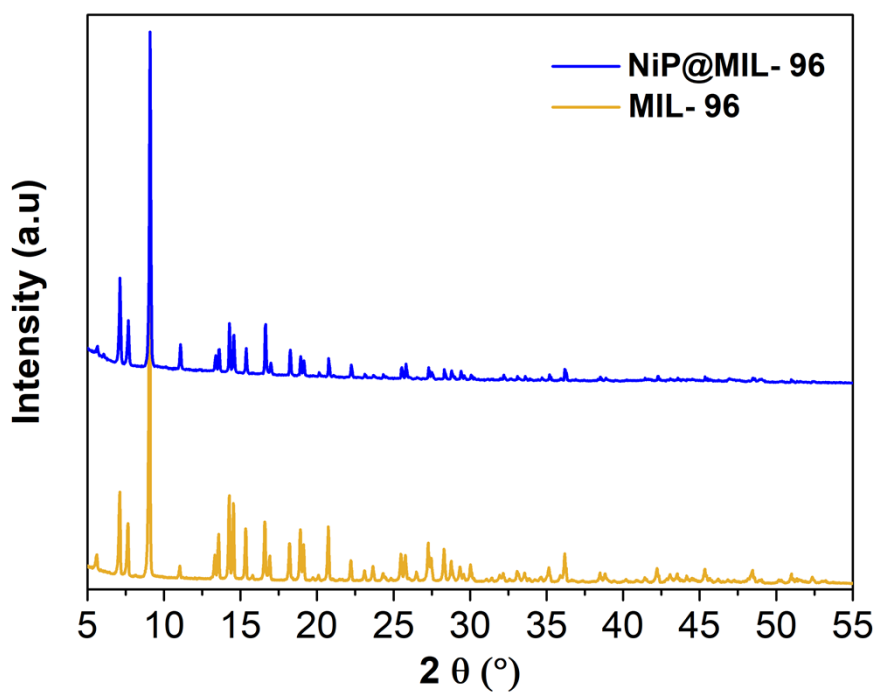


Fig.S1 XRD patterns of (a) MIL-96 and NiP-plated MIL-96

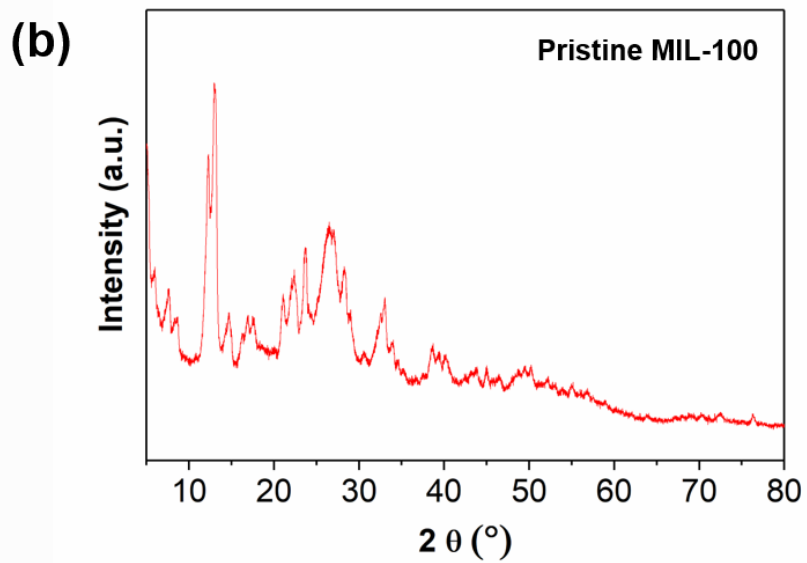
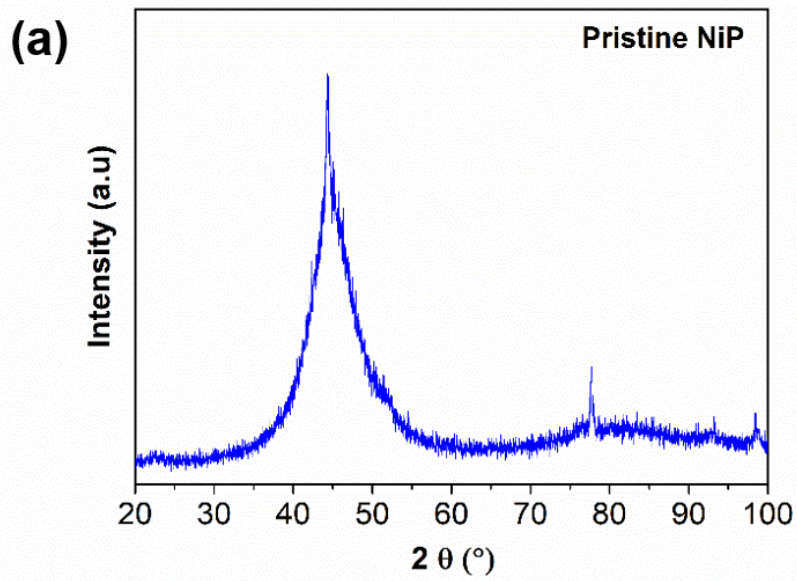


Fig. S2 XRD patterns of (a) pristine NiP-plating (b) pristine MIL-100

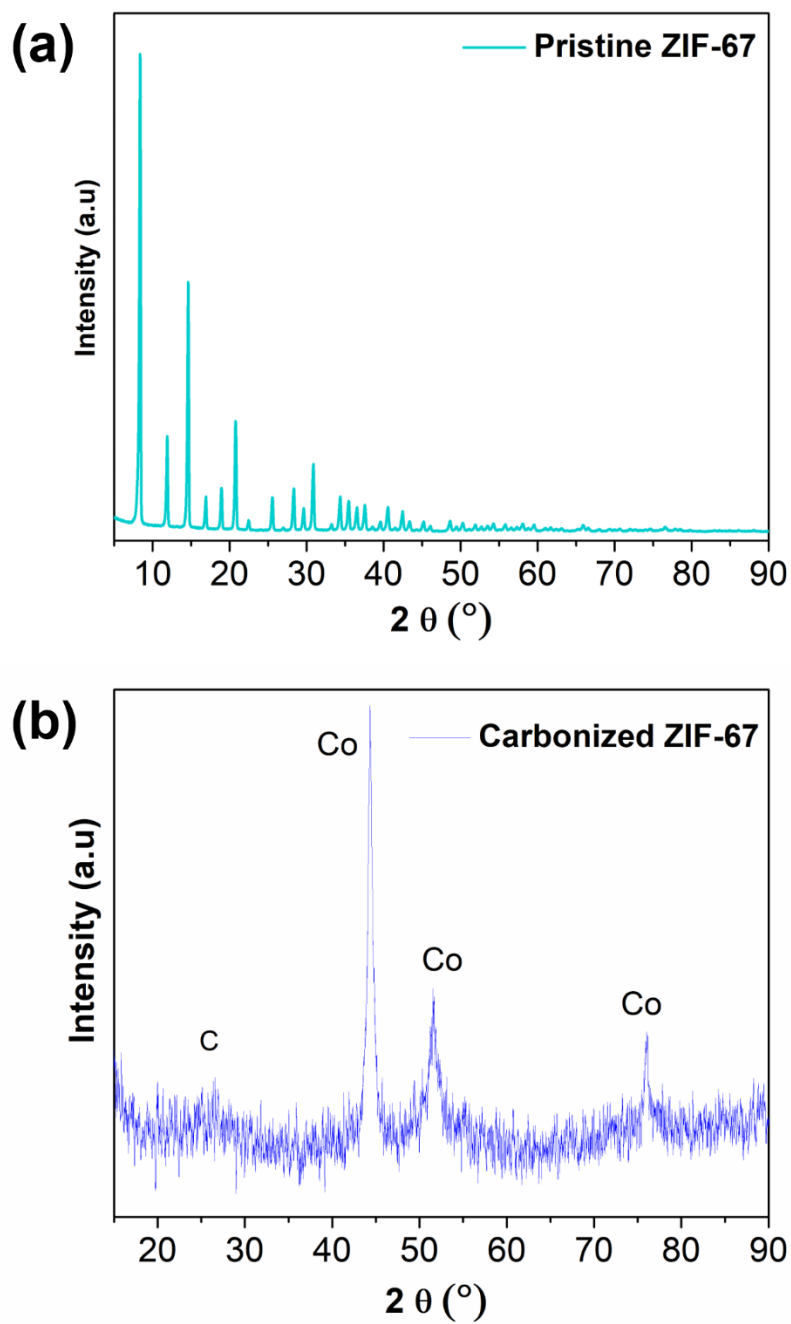


Fig.S3 XRD patterns of pristine ZIF-67 and (b) Carbonized ZIF-67 after the calcination of ZIF-67 at 750°C in the atmosphere of N_2 .

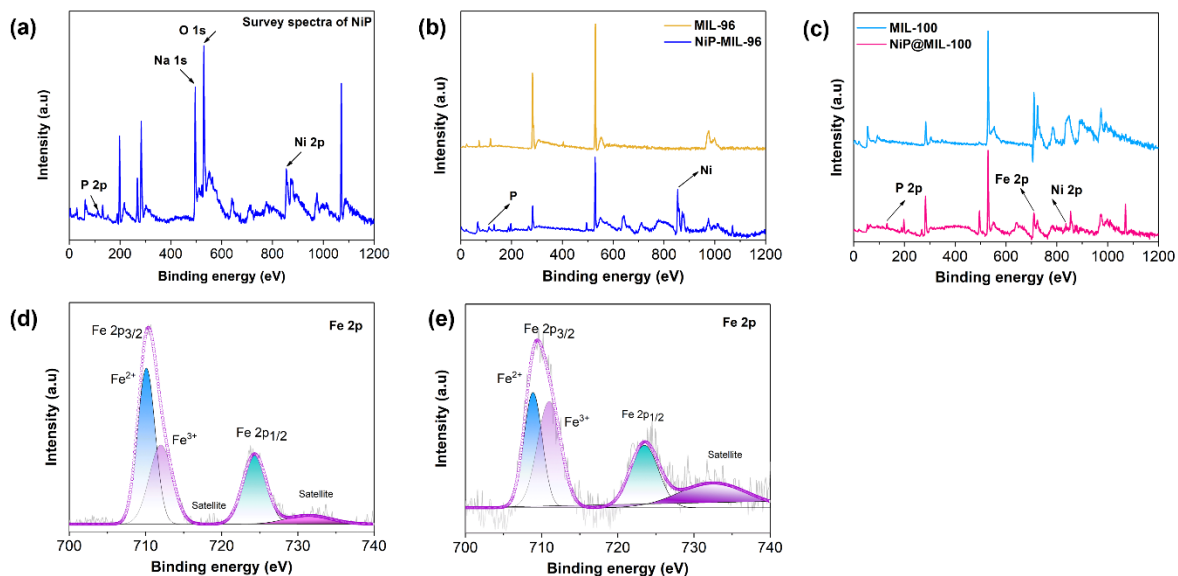


Fig. S4 Survey spectra of (a) pristine NiP, (b) pristine MIL-96 and NiP@MIL-96 and (c) pristine MIL-100 and NiP@MIL-100, High-resolution deconvoluted XPS spectrum of Fe 2p of (d) pristine MIL-100 and (e) NiP@MIL-100

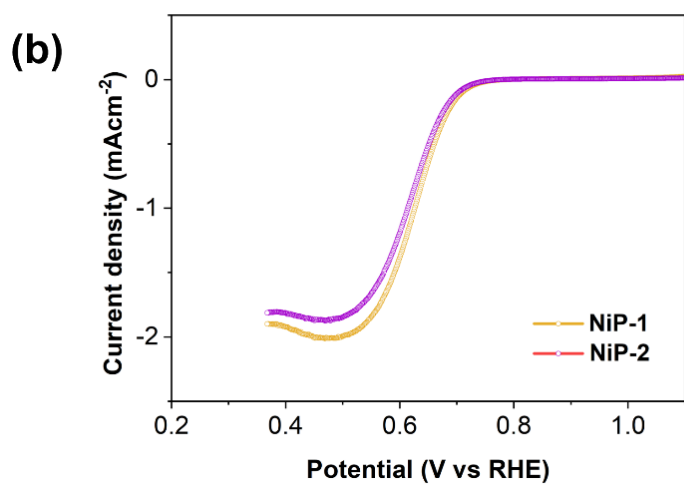
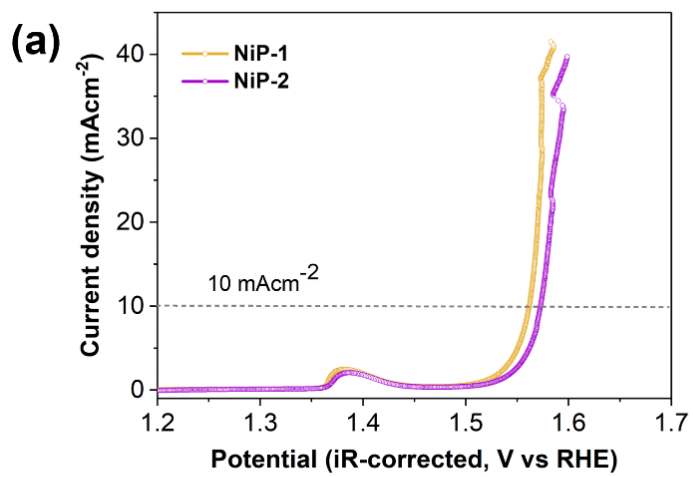


Fig. S5 (a) iR-corrected LSV curves of OER of NiP1 and NiP2 (b) LSV curves of ORR of NiP1 and NiP2

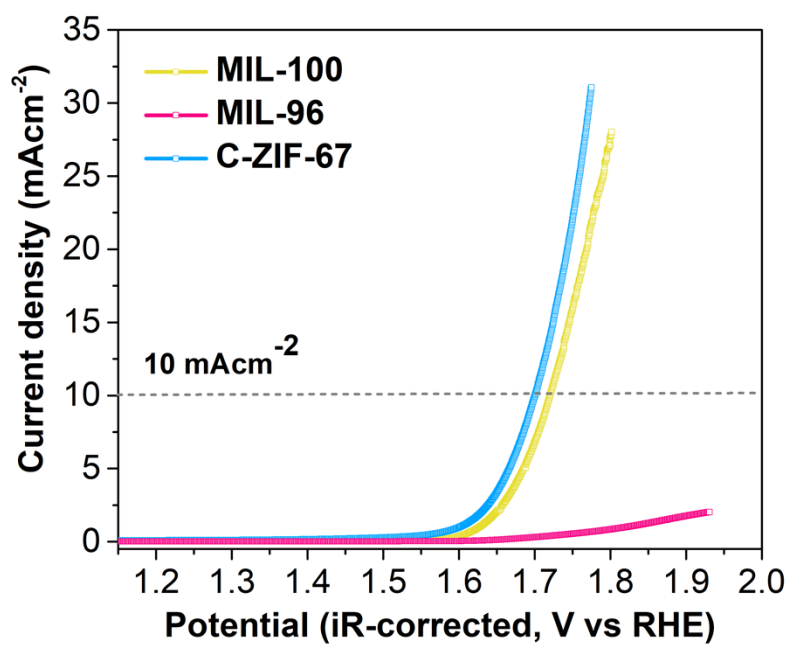


Fig. S6 iR-corrected LSV curves of OER of pristine MIL-96, MIL-100 and carbonized ZIF-67

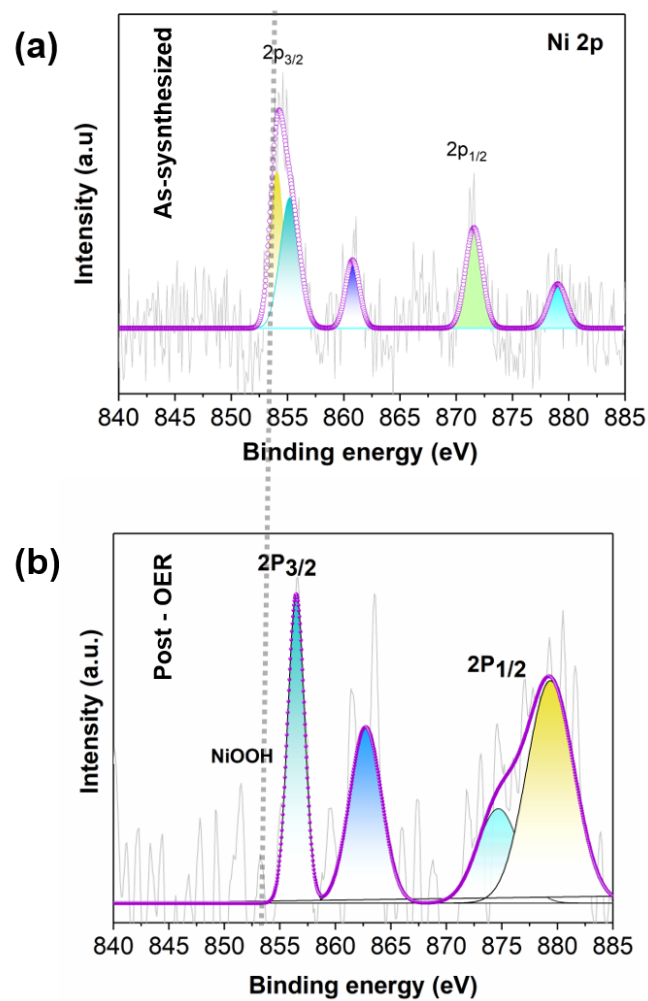


Figure S7. XPS characterization of Ni 2p in the NiP@MIL-100 (a) XPS spectra of the as-synthesized NiP@MIL-100, (b) XPS spectra of NiP@MIL-100 after OER activity, respectively.

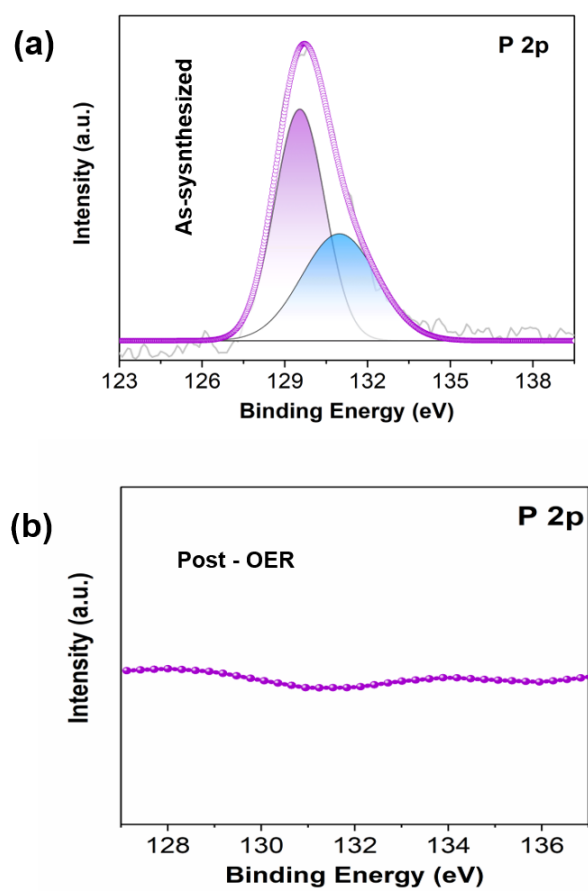


Figure S8. XPS characterization of P 2p in the NiP@MIL-100 (a) XPS spectra of the as-synthesized NiP@MIL-100, (b) XPS spectra of NiP@MIL-100 after OER activity, respectively.

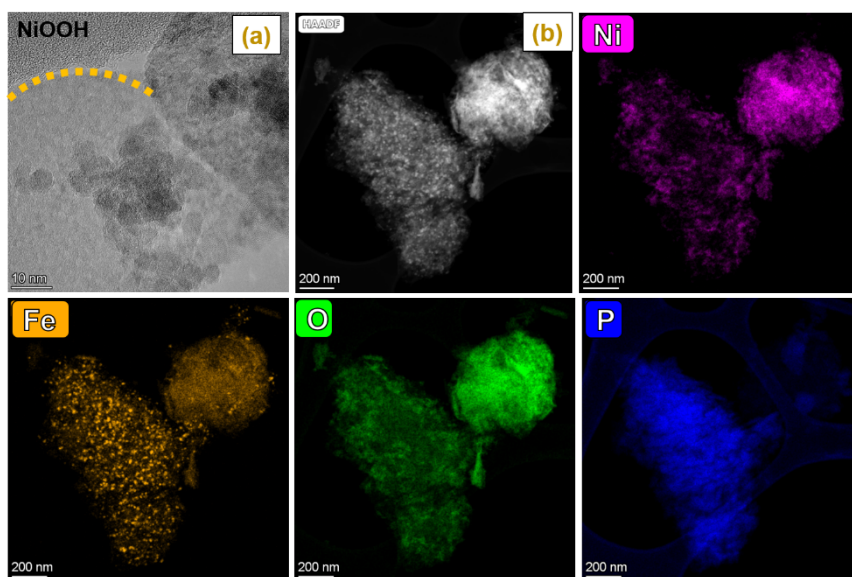


Fig. S9 TEM and HAADF-STEM images of spent NiP@MIL-100 sample after OER and its corresponding element mapping images.

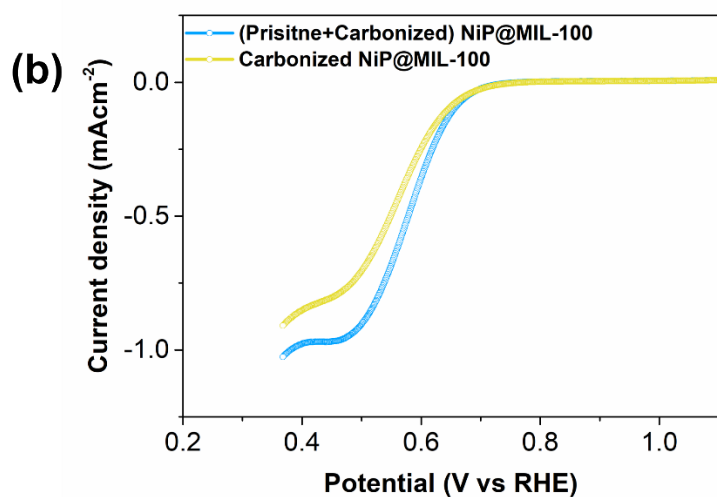
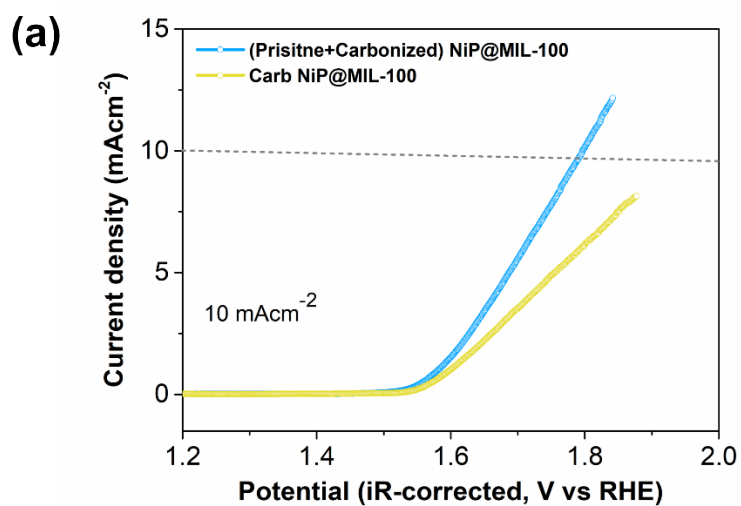


Fig. S10 (a) iR-corrected LSV curves of OER of carbonized NiP@MIL-100 and pristine +carbonized (50:50) NiP@MIL-100 catalysts in O_2 -saturated 0.10 M KOH solution at 1600 rpm; (b) LSV curves of ORR of carbonized NiP@MIL-100 and pristine +carbonized (50:50) NiP@MIL-100 catalysts in O_2 -saturated 0.10 M KOH solution at 1600 rpm

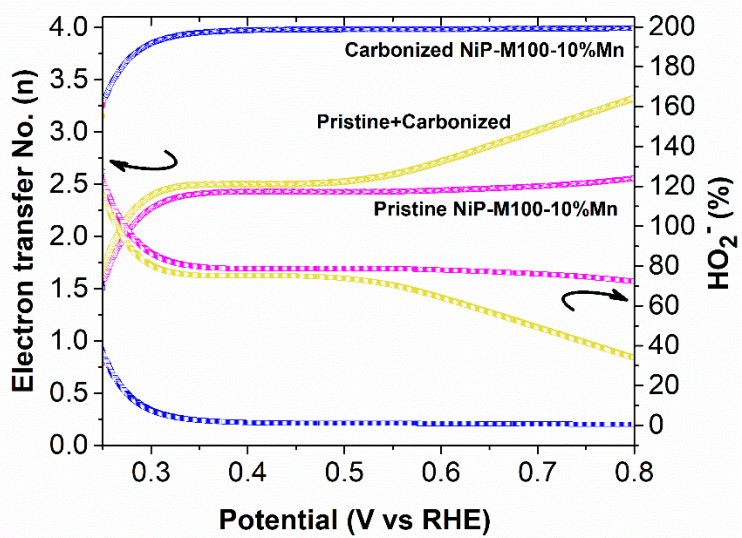


Fig. S11 Electron transfer number and percentage of HO_2^- of pristine NiP@MIL-100, carbonized NiP@MIL-100 and pristine +carbonized (50:50) NiP@MIL-100 catalysts.

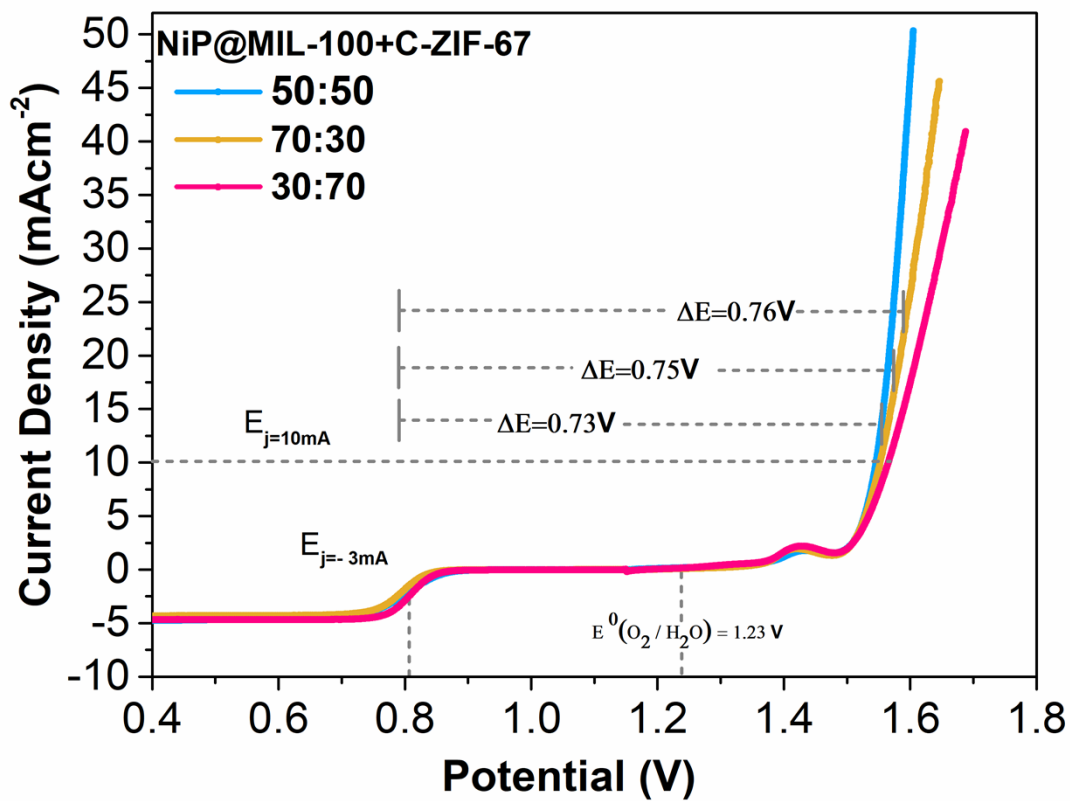


Fig. S12 Overall polarization curves of C-ZIF-67+NiP@MIL-100 at different ratios in 0.1 M KOH

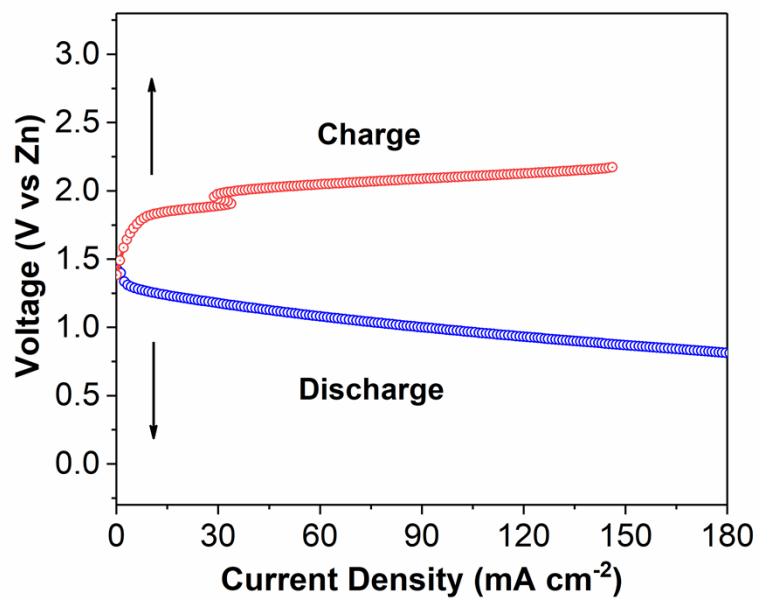


Fig. S13 Discharge and charge polarization curves

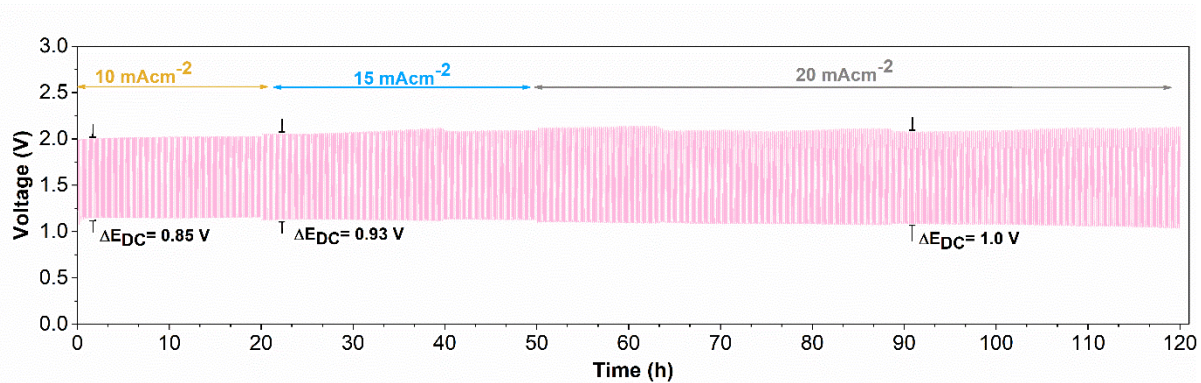


Fig. S14 Galvanostatic charge/discharge test for rechargeable zinc-air battery based on pristine NiP@MIL-100+ carbonized ZIF-67 tested for cyclic stability at 10, 15 and 20 mA cm⁻²

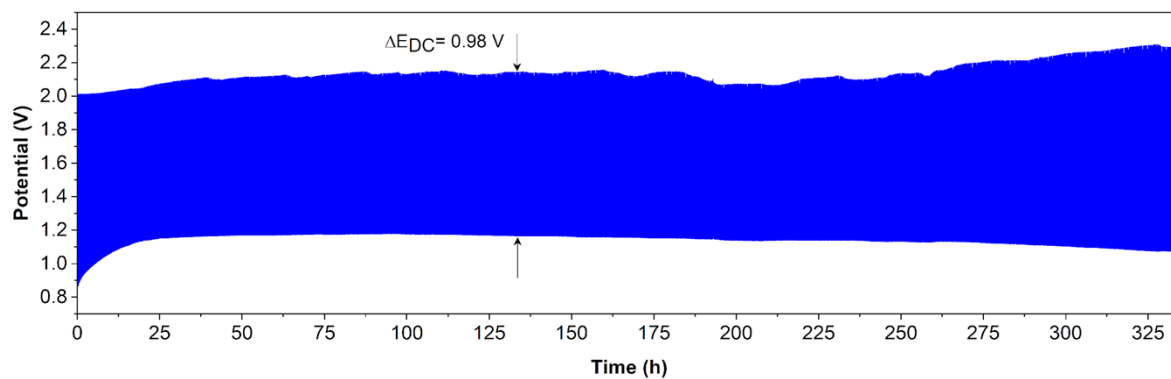


Fig. S15 Rechargeable zinc–air battery test. galvanostatic charge/discharge test based on pristine NiP@MIL-100 catalysts tested for cyclic stability at 5 mA cm^{-2} .

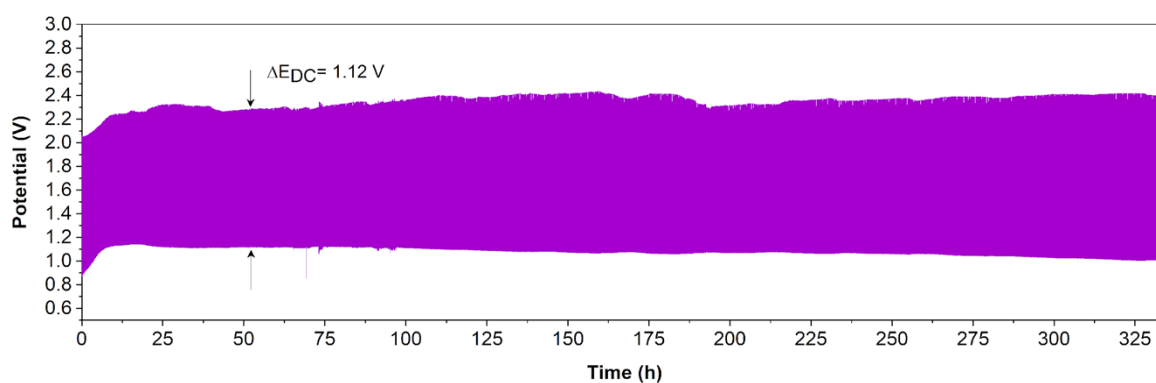


Fig. S16 Rechargeable zinc–air battery test. galvanostatic charge/discharge test based on carbonized NiP@MIL-100 catalysts tested for cyclic stability at 5 mA cm^{-2} .

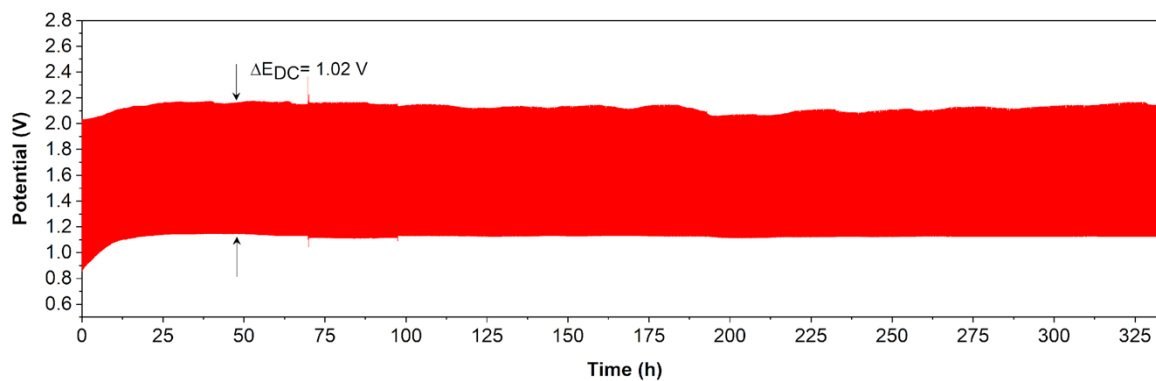


Fig. S17 Rechargeable zinc–air battery test. galvanostatic charge/discharge test based on pristine+carbonized (50:50) NiP@MIL-100 catalysts tested for cyclic stability at 5 mA cm^{-2} .

Table S1 BET surface area, pore volume and pore size of different materials.

Catalyst	Surface area (m²/g)	Pore volume (cm³/g)	Pore size (nm)
MIL-96	619.5	0.2180	1.74
NiP@MIL-96	11.2	0.0054	0.27
MIL-100	1,594.7	0.3676	1.77
NiP@MIL-100	6.1	0.0005	0.98

Table. S2 Peak positions of the samples before and after NiP-plating

Samples	Peak position of elements (eV)				
	Ni		P		Fe
	Ni ^{δ+}	Oxidized Ni	P ^{δ-}	Oxidized P	Fe ²⁺
Pristine NiP	853.82	855.15	130.5	132.4	-
NiP@MIL-96	853.80	855.14	130.5	132.35	-
MIL-100		-		-	710.1
NiP@MIL-100	854.75	855.3	129.6	131.2	708.6

Table S3 Performance comparison of OER, ORR and Zinc-air battery performance of recently published work.

Catalysts	Peak power density (mW cm⁻²)	Onset Potential V	E_{1/2} V	E_{j=10} V	ΔE= E_{j=10}-E_{1/2} V	Tafel slope mvdec⁻¹	Stability (h)	References
NiP@MIL-100+C-ZIF-67	203	0.94	0.83	1.52	0.69	62	500	This study
109CoNC SAC	162	1.05	0.86	1.65	0.79	-	80	1
NCA/Fe _{SA+NC}	236	1.12	0.92	1.57	0.65	71.5	300	2
Fe _{1.2} (CoNi) _{1.8} S ₆ MES	124	-	0.80	1.48	0.68	53.0	140	3
Fe, Ni@N-MWCNTs	114.9	0.84	0.71	1.54	0.83	40.0	170	4
Pt-NiO@Ni SP	188	1.04	0.90	1.55	0.65	97.3	200	5
CoP/CoO@MNC-CNT	152.8	0.921	0.84	1.50	0.66	89.3	500	6
Cu-Co/NC	295.9	0.97	0.85	1.49	0.64	60.4	500	7
Co-CoO/NPCF	214.1	0.91	0.843	1.59	0.75	43.8	200	8
CrMnFeCoNi	116.5	0.88	0.78	1.50	0.72	38	240	9
Co@C-CoNC	162.8	0.99	0.906	1.64	0.74	73	100	10
Fe SAs HS	170	1.0	0.86	1.57	0.71	68.8	70	11
NixP-NP-C900	266	0.90	0.76	1.78	1.02	205	20	12
S-CFZ	180	0.84	0.82	1.53	0.71	-	500	13
Co1-N3PS/HC	176	1.0	0.92	-	-	-	50	14
SA&NP-FeCo-NTS	108	0.98	0.85	1.58	0.73	109	250	15

CoFeN-NCNTs//CCM	145	0.89	0.84	1.57	0.73	49	500	16
NiFe ₃ @NGHS-NCNTs	126.5	-	0.83	1.62	0.79	-	166	17
Co/CoSe@NC	148	0.9	0.81	1.56	0.75	78	125	18
Co/CeO ₂ -NCNA@CC	123	-	0.77	1.58	0.81	-	380	19
FeNP@Fe-N-C	106.5	0.92	0.84	1.55	0.71	216	68	20
CC3	85	0.97	0.83	1.62	0.79	102	120	21
S-NiFe-LDH/NG	165	0.85	0.70	1.47	0.77	41	120	22
Ni-Fe-S/xNCQDs	94	0.97	0.85	1.53	0.68	86	240	23
Fe-FNC	226	0.85	0.80	-	-	-	140	24
Fe/12Zn/Co-NCNTs	166	1.0	0.88	1.57	0.69	93	320	25
Fe ₃ Co/DSA-NSC	240	0.96	0.88	1.45	0.57	62	60	26
Fe ₃ C/N,S-CNS	163	0.98	0.86	-	-	77	750	27
FeNi ₃ @NWC	143	-	0.84	1.52	0.68	-	266	28
Co@NSC	141	0.91	0.86	1.57	0.71	181	94	29
FeNi LDH-TpF6	118	-	-	-	-	-	800	30
CoCu/N-CNS	104.3	0.92	0.84	1.48	0.64	99	400	31
NPPC	173.8	0.97	0.87	-	-	-	300	32
FeCoP2-CN _C	76.9	0.91	0.85	1.53	0.68	124	45	33

References

1. C.-X. Zhao, J.-N. Liu, J. Wang, C. Wang, X. Guo, X.-Y. Li, X. Chen, L. Song, B.-Q. Li and Q. Zhang, *Science Advances*, 2022, **8**, eabn5091.
2. Y. Chen, T. He, Q. Liu, Y. Hu, H. Gu, L. Deng, H. Liu, Y. Liu, Y.-N. Liu, Y. Zhang, S. Chen and X. Ouyang, *Applied Catalysis B: Environmental*, 2023, **323**, 122163.
3. H. Wu, Z. Li, Z. Wang, Y. Ma, S. Huang, F. Ding, F. Li, Q. Zhai, Y. Ren, X. Zheng, Y. Yang, S. Tang, Y. Deng and X. Meng, *Applied Catalysis B: Environmental*, 2023, **325**, 122356.
4. Q. Jing, Z. Mei, X. Sheng, X. Zou, Y. Yang, C. Zhang, L. Wang, Y. Sun, L. Duan and H. Guo, *Chemical Engineering Journal*, 2023, **462**, 142321.
5. F. Zhang, R. Ji, X. Zhu, H. Li, Y. Wang, J. Wang, F. Wang and H. Lan, *Small*, **n/a**, 2301640.
6. H. W. Go, T. T. Nguyen, Q. P. Ngo, R. Chu, N. H. Kim and J. H. Lee, *Small*, 2023, **19**, 2206341.
7. Z. Li, S. Ji, C. Wang, H. Liu, L. Leng, L. Du, J. Gao, M. Qiao, J. H. Horton and Y. Wang, *Advanced Materials*, 2023, **35**, 2300905.
8. Y. Luo, M. Wen, J. Zhou, Q. Wu, G. Wei and Y. Fu, *Small*, **n/a**, 2302925.
9. R. He, L. Yang, Y. Zhang, X. Wang, S. Lee, T. Zhang, L. Li, Z. Liang, J. Chen, J. Li, A. Ostovari Moghaddam, J. Llorca, M. Ibáñez, J. Arbiol, Y. Xu and A. Cabot, *Energy Storage Materials*, 2023, **58**, 287-298.
10. S. Chandrasekaran, R. Hu, L. Yao, L. Sui, Y. Liu, A. Abdelkader, Y. Li, X. Ren and L. Deng, *Nano-Micro Letters*, 2023, **15**, 48.
11. Y. Wang, P. Meng, Z. Yang, M. Jiang, J. Yang, H. Li, J. Zhang, B. Sun and C. Fu, *Angewandte Chemie International Edition*, 2023, **62**, e202304229.
12. Y. Wang, J. Liu, T. Lu, R. He, N. Xu and J. Qiao, *Applied Catalysis B: Environmental*, 2023, **321**, 122041.
13. Y. Jiang, Y.-P. Deng, R. Liang, N. Chen, G. King, A. Yu and Z. Chen, *Journal of the American Chemical Society*, 2022, **144**, 4783-4791.
14. Y. Chen, R. Gao, S. Ji, H. Li, K. Tang, P. Jiang, H. Hu, Z. Zhang, H. Hao and Q. Qu, *Angew. Chem. Int. Ed.*, 2021, **60**, 3212-3221.
15. Q. Zhang, P. Liu, X. Fu, Y. Yuan, L. Wang, R. Gao, L. Zheng, L. Yang and Z. Bai, *Adv. Funct. Mater.*, 2022, **32**, 2112805.
16. G. Zhou, G. Liu, X. Liu, Q. Yu, H. Mao, Z. Xiao and L. Wang, *Adv. Funct. Mater.*, 2022, **32**, 2107608.
17. Y. Ma, W. Chen, Z. Jiang, X. Tian, X. WangGuo, G. Chen and Z.-J. Jiang, *J. Mater. Chem. A*, 2022, **10**, 12616-12631.
18. K. Li, R. Cheng, Q. Xue, P. Meng, T. Zhao, M. Jiang, M. Guo, H. Li and C. Fu, *Chem. Eng. J.*, 2022, **450**, 137991.
19. S. Li, H. Zhang, L. Wu, H. Zhao, L. Li, C. Sun and B. An, *J. Mater. Chem. A*, 2022, **10**, 9858-9868.
20. C. Yang, S. Shang, Q. Gu, J. Shang and X.-y. Li, *J. Energy Chem.*, 2022, **66**, 306-313.
21. C. Liu, F. Liu, H. Li, J. Chen, J. Fei, Z. Yu, Z. Yuan, C. Wang, H. Zheng, Z. Liu, M. Xu, G. Henkelman, L. Wei and Y. Chen, *ACS Nano*, 2021, **15**, 3309-3319.
22. X. Han, N. Li, J. S. Baik, P. Xiong, Y. Kang, Q. Dou, Q. Liu, J. Y. Lee, C. S. Kim and H. S. Park, *Advanced Functional Materials*, 2023, **33**, 2212233.
23. R. Wang, J. Liu, J. Xie, Z. Cai, Y. Yu, Z. Zhang, X. Meng, C. Wang, X. Xu and J. Zou, *Applied Catalysis B: Environmental*, 2023, **324**, 122230.
24. C. Xu, C. Guo, J. Liu, B. Hu, H. Chen, G. Li, X. Xu, C. Shu, H. Li and C. Chen, *Small*, **n/a**, 2207675.
25. J. Xue, S. Deng, R. Wang and Y. Li, *Carbon*, 2023, **205**, 422-434.
26. G. Yasin, S. Ali, S. Ibraheem, A. Kumar, M. Tabish, M. A. Mushtaq, S. Ajmal, M. Arif, M. A. Khan, A. Saad, L. Qiao and W. Zhao, *ACS Catalysis*, 2023, **13**, 2313-2325.
27. Q.-D. Ruan, R. Feng, J.-J. Feng, Y.-J. Gao, L. Zhang and A.-J. Wang, *Small*, **n/a**, 2300136.

28. Y. Wang, Y. Liu, L. Zhou, P. Zhang, X. Wu, T. Liu, S. Mehdi, X. Guo, J. Jiang and B. Li, *Journal of Materials Chemistry A*, 2023, **11**, 1894-1905.
29. X. Yan, Y. Tu, H. Yuan, Y. Xia, Y. Jiang, S. Zhu, C. Li, H. Tang, P. Du and M. Lei, *Advanced Composites and Hybrid Materials*, 2023, **6**, 71.
30. Q. Cao, L. Wan, Z. Xu, W. Kuang, H. Liu, X. Zhang, W. Zhang, Y. Lu, Y. Yao, B. Wang and K. Liu, *Advanced Materials*, **n/a**, 2210550.
31. J. Kuang, Y. Shen, Y. Zhang, J. Yao, J. Du, S. Yang, S. Zhang, Y. Fang and X. Cai, *Small*, **n/a**, 2207413.
32. C. Hu, Q. Liang, Y. Yang, Q. Peng, Z. Luo, J. Dong, T. T. Isimjan and X. Yang, *Journal of Colloid and Interface Science*, 2023, **633**, 500-510.
33. R. Liu, Y. Wang, W. Zheng, H. Zhang and Z. Zhang, *Energ Fuel*, 2023, **37**, 1344-1352.